Modeling and Simulation for Refueling Boom and Receiver in Coupled Mode

Yang Chaoxing[1], *Yang Yu*[2], *Lu Yuping*[1*]

1. College of Automation Engineering, Nanjing University of Aeronautics and Astronautics, Nanjing 211106, P. R. China

2. Shanghai Institute of Spaceflight Control Technology, Shanghai 200000, P. R. China

(Received 13 October 2015; revised 11 November 2015; accepted 12 December 2015)

Abstract: In coupled mode, the major problem of boom refueling system is undesirable nozzle loads. An automated load alleviation system (ALAS) is needed to alleviate nozzle loads. In order to simulate dynamic of the system and to validate ALAS, dynamic model is developed. Two models are established, which are the static model and the moving model, named after the two relative states between the fixed boom and the extension boom. Kane method is employed as main method considering system's multi-body characteristics. D'Alembert's principle is used to calculate nozzle loads. Simulation is conducted to research the effects of position disturbance and velocity disturbance on nozzle loads. Results indicate that position disturbance plays a more significant role in inducing nozzle loads. A fuzzy control law based ALAS is validated using the formulated model. It is concluded that this model can simulate system dynamic and validate ALAS.

Key words: applied mechanics; boom refueling; nozzle load; Kane method; multi-body system

CLC number: V212.2 **Document code**: A **Article ID**: 1005-1120(2017)02-0143-09

0 Introduction

Aerial refueling is the procedure of transferring fuel from a tanker to a receiver aircraft during flight. It allows the receiver to take off with a greater payload, remain airborne longer and extend its maximum range[1]. Aerial refueling is of great value for military because it significantly increases the efficiency of military aircraft. It is also promising in commercial use, for refueling a cargo airplane can obtain payload increase, range extension, and finally cost reduction[2]. Two methods commonly used for aerial refueling are boom and receptacle refueling (BRR) and probe and drogue refueling (PDR). Compared with PDR, BRR offers faster fuel transfer and is more suitable for large transport aircraft which is less agile but needs much more fuel.

Dynamic and control issues are different between free-flight mode and coupled mode of BRR system. In free-flight mode, motion of refueling boom has low damping ratio, and is influenced by motion of tanker, boom extension and wind disturbance. Although it is the boom operator's responsibility to move and extend the boom by wrist controller during docking process, a stability augmentation system (SAS) is required to enhance stability and handling quality. The process involves a few issues like multi-body system modeling, boom's SAS designing, attitudes dynamic decoupling and disturbance rejection control law designing[3-9].

In coupled mode, the major problem is the undesirable radial loads on nozzle, caused by the change of relative position between tanker and receiver. Nozzle loads must be limited in a low level to avoid destruction of refueling boom or receiver, and to ensure the safety of fuel transfer process. However, it appears impossible to null

* Corresponding author, E-mail address: yplac@nuaa.edu.cn.

How to cite this article: Yang Chaoxing, Yang Yu, Lu Yuping. Modeling and simulation for refueling boom and receiver in coupled mode[J]. Trans. Nanjing Univ. Aero. Astro., 2017,34(2):143-151.
http://dx.doi.org/10.16356/j.1005-1120.2017.02.143

out nozzle loads by manual operation, because the deformation of boom caused by nozzle loads is too tiny to be detected by eyes. Thus, an automated load alleviation system (ALAS) is required. In engineering, high-fidelity simulations and analyses are necessary for BRR system in coupled mode, especially for UAV's autonomous aerial refueling, because the latter introduces new tactical, operational, and safety issues which are not encountered in manned aircraft aerial refueling operation[4]. However, researches on coupled mode are rarely published, except Ref. [9] which only briefly discussed the configuration of ALAS.

Motivation for our study is to develop a generalized approach to simulate flight dynamic and to validate ALAS of BRR in coupled mode before test flight. The approach combines Kane method and D' Alembert's principle. The former is to derive equations of motion (EoMs) of the system and the latter to derive equations of nozzle loads. Then, the factors affecting nozzle loads are analyzed by simulation. Finally, an ALAS is simulated as an example to illustrate the usage of the approach.

1 Method

1.1 Kane method

Kane method is better at formulating EoMs for complex mechanical system than classical approaches such as Newton-Euler method and Lagrange method. We choose this method because of the multi-body characteristic of BRR system. After EoMs are all formulated, D' Alembert's principle is applied to formulate equations of nozzle loads.

Kane method employs generalized speeds to formulate EoMs of system. Generalized speeds is a group of variables, which are independent from one another and can be used to uniquely define the velocities and angular velocities of the system. The number of generalized speeds equals to that of independent dynamical equations, as well as the degrees of freedom (DoFs) of the system. In this paper, Kane method is described as briefly as possible. For more detailed information, please go to Ref. [10] or Ref. [11].

For a system with n rigid bodies and m DoFs, Kane's equations can simply be presented as a set of scalar equations

$$F^r + F^{*r} = 0 \quad r = 1, \cdots, m \tag{1}$$

where F^r is the generalized active force and F^{*r} the generalized inertia force with respect to the rth generalized speed u_r. F^r and F^{*r} can be written as

$$\begin{cases} F^r = \sum_{i=1}^{n} (\boldsymbol{F}_i \boldsymbol{V}_i^r + \boldsymbol{M}_i \boldsymbol{\omega}_i^r) \\ F^{*r} = \sum_{i=1}^{n} (\boldsymbol{F}_i^* \boldsymbol{V}_i^r + \boldsymbol{M}_i^* \boldsymbol{\omega}_i^r) \end{cases} \tag{2}$$

where i stands for the index of rigid bodies, $\boldsymbol{F}_i$ ($\boldsymbol{M}_i$) the active force (moment) on body i, $\boldsymbol{F}_i^*$ ($\boldsymbol{M}_i^*$) the inertia force (moment) of body i, $\boldsymbol{V}_i^r$ the partial velocity, and $\boldsymbol{\omega}_i^r$ partial angular velocity with respect to u_r. $\boldsymbol{V}$ and $\boldsymbol{\omega}_i^r$ are defined as

$$\begin{cases} \boldsymbol{V}_i^r = \dfrac{\partial \boldsymbol{V}_i}{\partial u_r} \\ \boldsymbol{\omega}_i^r = \dfrac{\partial \boldsymbol{\omega}_i}{\partial u_r} \end{cases} \tag{3}$$

where $\boldsymbol{V}_i$ stands for the velocity of mass center of body i, and $\boldsymbol{\omega}_i$ the angular velocity.

1.2 System description

BRR system in coupled mode, as shown in Fig. 1, is composed of four parts: Tanker, fixed boom (FB), extension boom (EB) and receiver. FB is attached to the tanker by a universal joint, which allows the boom's pitching and rolling controlled by boom elevator and rudder. EB is attached to receiver by spherical joint, allowing relative rotation in 3 directions. There are two states of EB, either relatively static, or extending (retracting) along FB when pulled (pushed) by receiver.

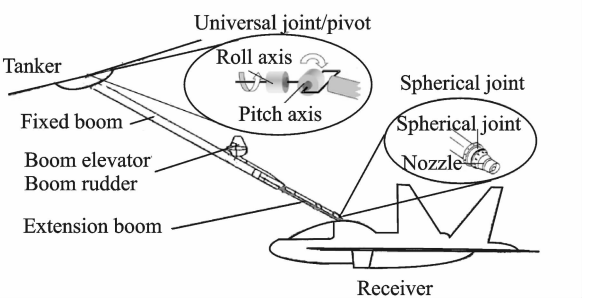

Fig. 1 Mechanical structure of BRR system in coupled mode

Coordinate systems are defined in Fig. 2. S_T and S_R correspond to the standard aircraft body frame (Origin is located at mass center. x-axis points forward, y-axis points starboard, and z-axis points down). The origin of S_B is located at pivot (universal joint). x-axis is parallel to longitudinal axis of flying boom and points from nozzle to pivot. y-axis is parallel to pitch axis of boom and points right when viewed from nozzle.

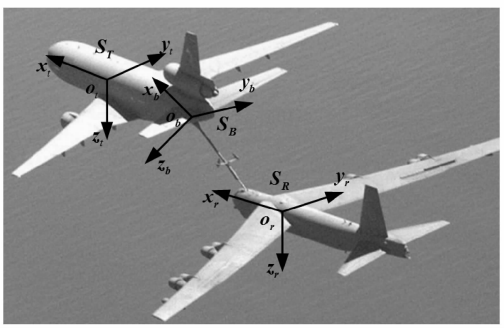

Fig. 2 Coordinate system definition

On the premise of coordinate systems defined, S_T is aligned with S_B by rotating about x-axis by angle ϕ firstly, then about y-axis by angle θ. ϕ and θ are defined as boom roll angle and pitch angle relative to tanker. S_R is aligned with S_B by rotating about z-axis by angle Ψ_t firstly, about y-axis by angle θ_t secondly and about x-axis by angle ϕ_t finally. θ_t, Ψ_t and ϕ_t are defined as boom pitch angle, yaw angle and roll angle relative to receiver. These variables, along with l, representing the length of EB outside of FB, are generalized coordinates of the system, which uniquely define the system's configuration.

Dynamic model is to be formulated under the following assumptions. (1) All components of system are rigid bodies. For clarity, index of FB (EB, receiver) is defined as Body 1 (Body 2, Body 3). (2) The tanker is in straight and level flight with constant speed. (3) Fuel transfer is not considered provisionally in this paper, so mass, mass center and inertia matrix of each rigid body remain constant in its own body frame. (4) Universal joint and spherical joint are assumed to be ideal joints without damping moments. Their detailed structures are not considered. They are abstracted as the points connecting adjacent rigid bodies and allowing the corresponding relative rotations. Nozzle loads are abstracted as the concentrated constraint forces on the corresponding point.

2 Dynamic Model Formulation

2.1 Model formulation with static EB

When EB is relatively static, the system is with five DoFs. Five generalized speeds are employed to formulate EoMs. We define $\boldsymbol{\omega}_a$ as relative angular velocity of the boom with respect to the tanker, and $\boldsymbol{\omega}_b$ as relative angular velocity of the boom with respect to the receiver. Generalized speeds are defined by components of $\boldsymbol{\omega}_a$ and $\boldsymbol{\omega}_b$ in S_B: u_1 and u_2 stand for y- and z-components of $\boldsymbol{\omega}_a$. u_3, u_4 and u_5 stand for x-, y- and z-components of $\boldsymbol{\omega}_b$.

Other parameters are defined as follows: m_1 (m_2, m_3) and $\boldsymbol{J}_1$ ($\boldsymbol{J}_2$, $\boldsymbol{J}_3$) represent mass and inertia matrix of FB(EB, receiver) to its mass center in S_B. Vector $\boldsymbol{r}_a$ points from pivot to mass center of FB, $\boldsymbol{r}_b$ points from pivot to mass center of EB, $\boldsymbol{r}_c$ points from mass center of EB to nozzle, and $\boldsymbol{r}_d$ points from nozzle to mass center of receiver. $\boldsymbol{V}_0$ represents the velocity of pivot. These parameters are constant except $\boldsymbol{r}_b$, $\boldsymbol{r}_d$ and $\boldsymbol{J}_3$. $\boldsymbol{r}_b$ is the function of l and is time-varying with EB moving. $\boldsymbol{r}_d$ and $\boldsymbol{J}_3$ are time-varying in S_B because of relative angular velocity between the receiver and the boom.

To derive $\boldsymbol{V}_i^r$ and $\boldsymbol{\omega}_i^r$, $\boldsymbol{V}_i$ and ω_i should be expressed in terms of the generalized speeds. In S_B, velocity of mass center of FB is

$$\boldsymbol{V}_1 = \boldsymbol{V}_0 + \boldsymbol{\omega}_a \times \boldsymbol{r}_a = \boldsymbol{V}_0 + \sum_{r=1}^{5} u_r \boldsymbol{V}_1^r \tag{4}$$

Angular velocity of FB is

$$\boldsymbol{\omega}_1 = \boldsymbol{\omega}_a = \sum_{r=1}^{5} u_r \boldsymbol{\omega}_1^r \tag{5}$$

Velocity of mass center of EB is

$$\boldsymbol{V}_2 = \boldsymbol{V}_0 + \boldsymbol{\omega}_a \times \boldsymbol{r}_b = \boldsymbol{V}_0 + \sum_{r=1}^{5} u_r \boldsymbol{V}_2^r \tag{6}$$

Angular velocity of EB is

$$\boldsymbol{\omega}_2 = \boldsymbol{\omega}_a = \sum_{r=1}^{5} u_r \boldsymbol{\omega}_2^r \tag{7}$$

Velocity of mass center of the receiver is

$$\boldsymbol{V}_3 = \boldsymbol{V}_0 + \boldsymbol{\omega}_a \times (\boldsymbol{r}_b + \boldsymbol{r}_c) + (\boldsymbol{\omega}_a - \boldsymbol{\omega}_b) \times \boldsymbol{r}_d = \boldsymbol{V}_0 + \sum_{r=1}^{5} u_r \boldsymbol{V}_3^r \tag{8}$$

Angular velocity of receiver is

$$\boldsymbol{\omega}_3 = \boldsymbol{\omega}_a - \boldsymbol{\omega}_b = \sum_{r=1}^{5} u_r \boldsymbol{\omega}_3^r \tag{9}$$

Partial velocities $\boldsymbol{V}_i^r$ and $\boldsymbol{\omega}_i^r$ are derived by substituting Eqs. (4)—(9) into Eq. (3).

$\boldsymbol{F}_1$ is composed of gravity and aerodynamic force. $\boldsymbol{M}_1$ is the aerodynamic moment. Components of $\boldsymbol{F}_2(\boldsymbol{M}_2)$ are the same as that of $\boldsymbol{F}_1(\boldsymbol{M}_1)$. $\boldsymbol{F}_3$ is composed of gravity, aerodynamic force, and propulsion. $\boldsymbol{M}_3$ is the aerodynamic moment on the receiver. In S_B, inertia force and moment of each body can be expressed as

$$\begin{cases} \boldsymbol{F}_1^* = -m_1 \dfrac{\partial \boldsymbol{V}_1}{\partial t} - m_1 \boldsymbol{\omega}_1 \times \boldsymbol{V}_1 \\ \boldsymbol{M}_1^* = -\boldsymbol{J}_1 \dfrac{\partial \boldsymbol{\omega}_1}{\partial t} - \boldsymbol{\omega}_1 \times \boldsymbol{J}_1 \boldsymbol{\omega}_1 \\ \boldsymbol{F}_2^* = -m_2 \dfrac{\partial \boldsymbol{V}_2}{\partial t} - m_2 \boldsymbol{\omega}_1 \times \boldsymbol{V}_2 \\ \boldsymbol{M}_2^* = -\boldsymbol{J}_2 \dfrac{\partial \boldsymbol{\omega}_2}{\partial t} - \boldsymbol{\omega}_1 \times \boldsymbol{J}_2 \boldsymbol{\omega}_2 \\ \boldsymbol{F}_3^* = -m_3 \dfrac{\partial \boldsymbol{V}_3}{\partial t} - m_3 \boldsymbol{\omega}_1 \times \boldsymbol{V}_3 \\ \boldsymbol{M}_3^* = -\boldsymbol{J}_3 \dfrac{\partial \boldsymbol{\omega}_3}{\partial t} - \dfrac{\partial \boldsymbol{J}_3}{\partial t} \boldsymbol{\omega}_3 - \boldsymbol{\omega}_1 \times \boldsymbol{J}_3 \boldsymbol{\omega}_3 \end{cases} \tag{10}$$

In the sixth equation of Eq. (10), partial derivative of $\boldsymbol{J}_3$ with respect to t should not be ignored, because $\boldsymbol{J}_3$ is time-varying in S_B.

F^r and F^{*r} are derived by substituting all $\boldsymbol{V}_i^r$, $\boldsymbol{\omega}_i^r$, $\boldsymbol{F}_i$, $\boldsymbol{M}_i$, $\boldsymbol{F}_i^*$ and $\boldsymbol{M}_i^*$ into Eq. (2). Then a set of scalar equations are derived by substituting F^r and F^{*r} into Eq. (1). Because of their complexity, we describe the normalized form rather than the detail expressions of these equations. They are in the form of

$$\sum_{r=1}^{5} A_{pr} \dot{u}_r = B_p \quad p = 1, 2, \cdots, 5 \tag{11}$$

where $\dot{u}_r$ are introduced in Eq. (10) in the process of derivative of $\boldsymbol{V}_i$ or $\boldsymbol{\omega}_i$. Parameters A_{pr} are functions of generalized coordinates, masses and inertia matrixes of rigid bodies. Parameters B_p are functions of generalized speeds and active forces, besides those of A_{pr}. For system researched here, the matrix $[A_{pr}]_{m \times m}$ is both symmetric and invertible, so that these equations are readily to be solved. To complete the set of EoMs, the following kinematic equations are included

$$\begin{cases} \dot{\theta} = u_1 \\ \dot{\phi} = u_2 \csc\theta \\ \dot{\theta}_t = u_4 \cos\phi_t - u_5 \sin\phi_t \\ \dot{\Psi}_t = (u_5 \cos\phi_t + u_4 \sin\phi_t) \sec\theta_t \\ \dot{\phi}_t = u_3 + (u_5 \cos\phi_t + u_4 \sin\phi_t) \tan\theta_t \end{cases} \tag{12}$$

2.2 Model formulation with EB moving

When EB moves, the DoFs of system is six. Besides those defined in Section 2.1, another generalized speed, $u_6 = \dot{l}$, representing the extending speed of EB, is employed. Procedure to derive EoMs is the same except that partial velocities and partial angular velocities with respect to u_6 should be considered. In S_B, $\boldsymbol{V}_i$ and $\boldsymbol{\omega}_i$ are expressed as

$$\begin{cases} \boldsymbol{V}_1 = \boldsymbol{V}_0 + \boldsymbol{\omega}_a \times \boldsymbol{r}_a \\ \boldsymbol{\omega}_1 = \boldsymbol{\omega}_a \\ \boldsymbol{V}_2 = \boldsymbol{V}_0 + \dfrac{\partial \boldsymbol{r}_b}{\partial t} + \boldsymbol{\omega}_a \times \boldsymbol{r}_b \\ \boldsymbol{\omega}_2 = \boldsymbol{\omega}_a \\ \boldsymbol{V}_3 = \boldsymbol{V}_0 + \dfrac{\partial \boldsymbol{r}_b}{\partial t} + \boldsymbol{\omega}_a \times (\boldsymbol{r}_b + \boldsymbol{r}_c) + (\boldsymbol{\omega}_a - \boldsymbol{\omega}_b) \times \boldsymbol{r}_d \\ \boldsymbol{\omega}_3 = \boldsymbol{\omega}_a - \boldsymbol{\omega}_b \end{cases} \tag{13}$$

By substituting Eq. (13) into Eq. (3), $\boldsymbol{V}_i^r$ and $\boldsymbol{\omega}_i^r$ are derived. Obviously, u_6 is introduced in the process of derivative of $\boldsymbol{r}_b$.

Components of active forces and expressions of inertial forces are basically the same as discussed in Section 2.1. The difference is that interaction force $\boldsymbol{F}_{12}^{\triangle}$ between FB and EB is active force now and should be considered. Subscript means that $\boldsymbol{F}_{12}^{\triangle}$ is on Body 2 from Body 1. Therefore, $\boldsymbol{F}_{12}^{\triangle}$ should be added to $\boldsymbol{F}_2$ and $-\boldsymbol{F}_{12}^{\triangle}$ should be added to $\boldsymbol{F}_1$.

$\boldsymbol{F}_{12}^{\triangle}$ points along x_b- axis in the negative direction of u_6 and its absolute value is

$$|\boldsymbol{F}_{12}^{\triangle}| = F_0 + F_k |u_6| \tag{14}$$

where F_0 represents the minimum force along x_b-axis to move EB and $F_k |u_6|$ the drag induced by relative speed. F_0 and F_k are constants and determined by mechanism and actuator between EB

and FB.

Then six scalar equations are derived in the form of

$$\sum_{r=1}^{6} A'_{pr}\dot{u}_r = B'_p \quad p=1,2,\cdots,6 \tag{15}$$

where A'_{pr} and B'_p are functions of the same parameters discussed in Section 2.1. To complete the set of EoMs, Eq. (12) and

$$\dot{l} = u_6 \tag{16}$$

are included.

2.3 Procedure of model switch

In coupled mode, the state of EB changes between relatively static and moving, with the changes of system states and forces on system. Therefore, the model should be switched when necessary.

When EB is relatively static, interaction force $\boldsymbol{F}_{12}$ between EB and FB is the constraint force. $\boldsymbol{F}_{12}$ can be employed to determine whether to switch the model or not. Applying D′ Alembert′s principle to receiver and EB, $\boldsymbol{F}_{12}$ can be expressed as

$$\boldsymbol{F}_{12} = -\boldsymbol{F}_3 - \boldsymbol{F}_3^* - \boldsymbol{F}_2 - \boldsymbol{F}_2^* \tag{17}$$

F_{12}^x, the x-component of $\boldsymbol{F}_{12}$ in S_B is what we need. EB turns to moving on condition that $|F_{12}^x|$ becomes larger than F_0.

EB turns from moving to relatively static only on condition that u_6 decreases to zero. If u_6 decreases to zero, EB is assumed to be static and F_{12}^x is calculated. EB will turn to static if $|F_{12}^x|$ is smaller than F_0, while it will keep moving if $|F_{12}^x|$ is not. In computer simulation, the condition that u_6 decreases to zero, will hardly be met because of the computational accuracy limitation. Therefore, a similar but weaker condition, that the sign of u_6 changes and its absolute value is smaller than a threshold value, is employed instead.

2.4 Equation of nozzle loads

With models formulated above, it is already able to simulate the dynamic of system. However, in order to validate ALAS, equations of nozzle loads must be derived. Under rigid-body assumption, nozzle loads are the constrain forces acting on nozzle exactly. Applying D′ Alembert′s principle to the receiver, we obtain

$$\boldsymbol{F}_{23} = -\boldsymbol{F}_3 - \boldsymbol{F}_3^* \tag{18}$$

x-, y- and z-component of $-\boldsymbol{F}_{23}$ in S_B are nozzle loads f_x, f_y and f_z we need. ALAS will null out f_y and f_z, if it is well designed.

3 Simulation

Simulation is conducted in Matlab/Simulink with block diagram in Fig. 3. Dynamic module calculates the derivatives of system states and judges whether to do the model switch. Active force module calculates the aerodynamic forces of the system, thrust of the receiver, gravity of each rigid body, etc, according to system states and deflections of actuators.

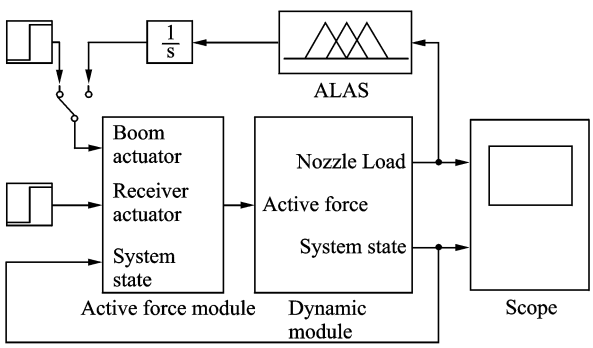

Fig. 3 Simulation block diagram

The height, speed of pivot and deflections of receiver actuators are artificially obtained. Deflections of boom actuators are obtained artificially, or by ALAS. ALAS used in simulation employs a fuzzy control law to calculate deflection rate of boom elevator (rudder), using the signal of $f_z(f_y)$. Under control of ALAS, actuators are always deflected to decrease nozzle loads. For example, if f_z is positive, the elevator is negatively deflected to decrease lift force on boom in order to null out f_z. Control law employed is designed by the basic fuzzy control theory. That is, the larger the nozzle loads are, the faster the actuators are deflected.

Initial states of system are set as follows: Height of pivot is 6 000 m, speed is Mach 0.7, and mass center of the receiver is 15 m behind and 8 m below the pivot. After trimming, nozzle

loads are nearly zero. θ is about 33.7°, θ_t about 32.1°, and l about 0.92 m.

3.1 Comparison of two models

Two models formulated are simulated separately without switch. The thrust of the receiver is decreased about 5%. Time histories of θ, l, f_x and f_z are shown in Fig. 4.

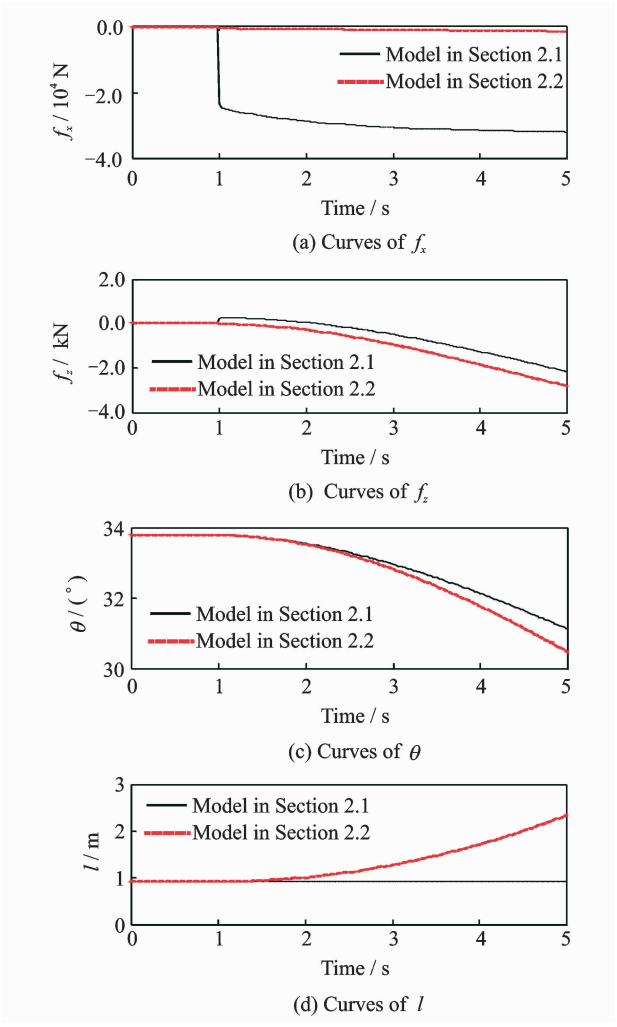

Fig. 4 Comparison of boom response and nozzle load between the two models

It shows that f_x is much larger if relative motion between EB and FB is forbidden. Nozzle load is so large and obviously unreasonable in practice. Therefore, the models used in simulation are necessary to be switched according to system's states and forces on the system. It also shows that differences between responses of the two models become larger and larger as time goes. When thrust decreases, the receiver decelerates so that the horizontal distance between itself and the tanker increases, which decreases θ in this simulation and finally makes EB to extend if allowed.

3.2 Effect of disturbance on nozzle loads

The effect of displacement disturbance on nozzle loads is simulated. This disturbance is added to simulation by recalculating initial values of the generalized coordinates according to the new position. Time histories of nozzle loads are shown in Fig. 5(a) when the new position of the receiver is set to 0.1 m/0.5 m/1 m lateral right relative to its trimming position, and in Fig. 5(b) when set to −0.3 m/0.3 m/0.5 m vertical down one by one.

Figs. 5(a, b) show that nozzle loads are significantly influenced by the displacement disturbance. The main reason might be the significant change of aerodynamic force on boom in a new position. For example, when the 0.5 m vertical down displacement is set to the receiver, the boom pitch angle θ is bigger than the trimming state, which induces a negative increase of aerodynamic pitch moment on the boom to decrease θ. Nozzle load f_z, the constrain force on nozzle, will hinder decreasing of θ. Consequently, f_z is required to be positive to induce a positive pitch moment on the boom, which is validated by the dotted-line of f_z in Fig. 5(b). In addition, model switching is observed from dotted-line of f_x in Fig. 5(b), where EB changes from static to moving, then to static again.

Effect of receiver's velocity disturbance is simulated. This disturbance is added to simulation by recalculating initial values of generalized speeds according to the new velocity. Time histories of nozzle loads are shown in Fig. 6(a) when new velocity is set to 0.1 m/s, −0.1 m/s and −0.2 m/s horizontal forward relative to its trimming state, and in Fig. 6(b) when set to 0.1 m/s, 0.2 m/s and 0.3 m/s lateral right one by one.

In this simulation, nozzle loads tend to hinder the changes of boom's angular velocity. For example, when 0.1 m/s horizontal forward is set to simulation, u_1 is positive and θ will increase

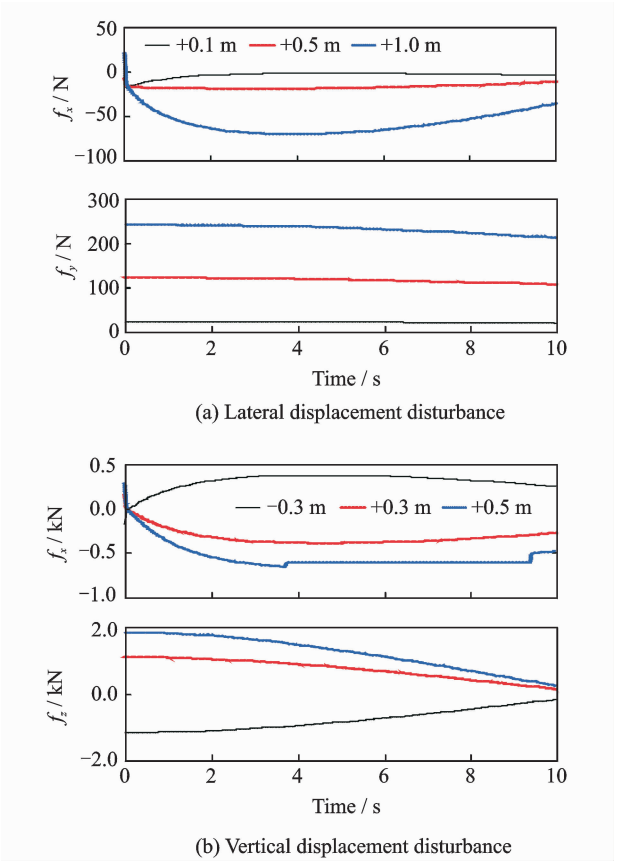

Fig. 5 Nozzle loads to displacement disturbances

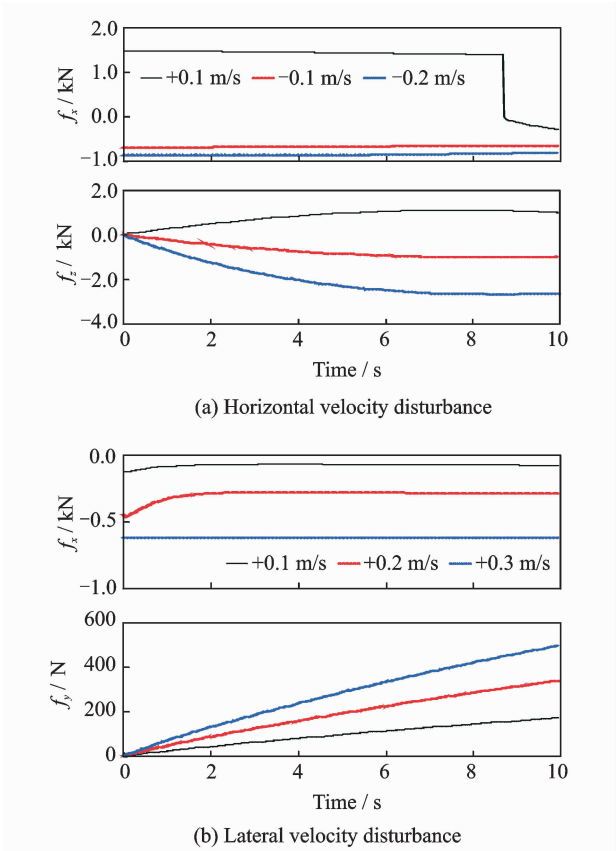

Fig. 6 Nozzle loads to velocity disturbances

compared with trimming state. Increasing θ induces negative increase of aerodynamic pitch moment on boom, which makes u_1 to decrease. Consequently, positive f_z is needed to induce positive pitch moment to hinder decreasing of u_1, which is validated by the solid-line of f_z in Fig. 5(a).

It shows that in the beginning of simulation, although velocity disturbances are different, nozzle loads are nearly the same. But after a period of time, nozzle loads become different, because the boom and the receiver have moved to different positions. It is implied that displacement disturbance plays a more significant role in inducing nozzle loads. The reason might be that aerodynamic force on system is significantly changed by displacement disturbance.

3.3 Simulation with ALAS

System with ALAS is simulated to show the usage of model formulated. Displacement disturbance −0.1 m vertical down, and velocity disturbance 0.1 m/s lateral right of receiver are added to simulation simultaneously. Nozzle loads are shown in Fig. 7 between simulation with and without ALAS. In Fig. 7, δ_e represents the boom elevator's deflection angle and δ_r the boom rudder's deflection angle.

Fig. 7 shows that actuators are deflected by ALAS to null out nozzle loads. When f_z is negative, δ_e is positively deflected, and when f_y is positive, δ_r is positively deflected. $f_y$and f_z are rapidly alleviated to a much lower level under the control of ALAS. Obviously, with the outputs of nozzle loads, models formulated are capable to validate ALAS in engineering.

It is necessary to point out that ALAS will not stabilize the states of system, because it is just designed to null out the nozzle loads. Fig. 8 shows time histories of θ and ϕ in this simulation. It is obvious that although f_z and f_y are nulled out, θ and ϕ are not stabilized. The reason is that the receiver is not under control. In an actual BRR process, the automatic control system or the pilot of the receiver will stabilize receiver's posi-

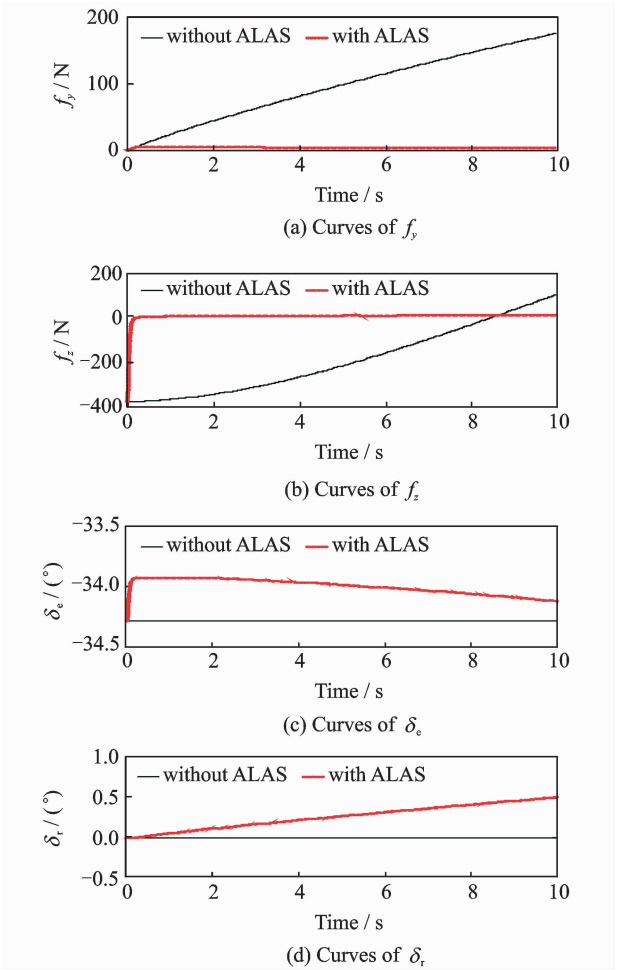

Fig. 7 Comparison of nozzle loads between system with and without ALAS

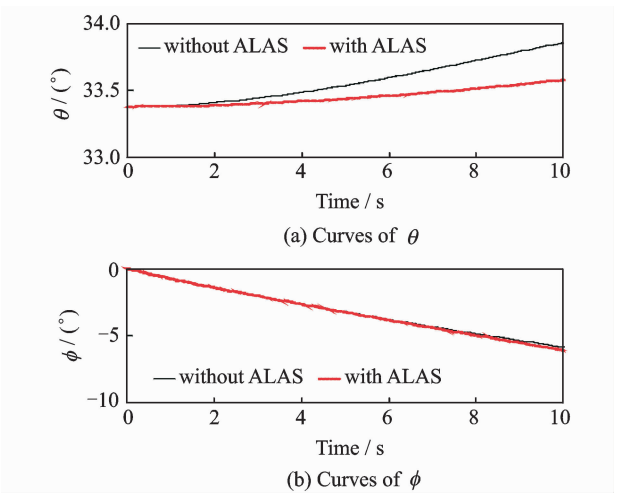

Fig. 8 Boom pitch angle and roll angle relative to the tanker

tion relative to the tanker. States such as θ and ϕ will be stabilized in that case.

4 Conclusions

We formulate a dynamic model of BRR system in coupled mode for simulation and ALAS validation. Dynamic model is formulated to reflect the multi-body and multi-model switching characteristics of the system. Simulation results indicate the necessity to switch between the two models. It is also indicated that the main factor inducing nozzle loads is the displacement disturbance. Velocity disturbance induces nozzle loads if the change of relative position becomes large enough after a period of time. Capability to send signals of nozzle loads makes model formulated available in ALAS verification and validation.

Acknowledgement

This work was supported by the National High Technology Research and Development Program ("863" Program) of China (No. 2013AA7052002).

References:

[1] MAO W, EKE F O. A survey of the dynamics and control of aircraft during aerial refueling [J]. Nonlinear Dynamic System Theory, 2008, 8(4): 375-388.

[2] BENNINGTON M A, VISSER K D. Aerial refueling implications for commercial aviation [J]. Journal of Aircraft, 2005, 42(2): 366-375.

[3] SMITH J J, KUNZ D L. Simulation of the dynamically coupled KC-135 tanker and refueling boom: AIAA 2007-6711[R]. USA: AIAA, 2007.

[4] SMITH A L, KUNZ D L. Dynamic coupling of the KC-135 tanker and boom for modeling and simulation [J]. Journal of Aircraft, 2007, 44(3): 1034-1039.

[5] YANG Chaoxing, LU Yuping. Kane method based modeling and analysis on multi-body dynamic of boom refueling system [J]. Journal of Nanjing University of Aeronautics & Astronautics, 2013, 45(3): 605-610. (in Chinese)

[6] QU Y H, CHEN L S, QIU J. Application of non-cancellation decoupling in boom refueling control [C]// 2009 IEEE International Conference on Mechatronics and Automation. New York, USA: IEEE, 2009: 4203-4207.

[7] HEI Wenjing, AN Gang, LIN Hao, et al. Input-output feedback non-linearization used in design of boom airrefueling control system [J]. Acta Aeronautica et Astronautica Sinica, 2008, 29(3): 651-656. (in Chinese)

[8] BEKEMEYER L G. Validation of the KC-10 refueling boom digital control system: SAE Technical Paper Series 821421[R]. USA: SAE, 1982.

[9] RIET R, THOMAS F R. KC-10A refueling boom control system [R]. Long Beach, California: Douglas Aircraft Company, McDonnell Douglas Corporation, 1980.

[10] BOLENDER M A. Rigid multi-body equations-of-motion for flapping wing MAVs using Kane′s equations: AIAA-2009-6158[R]. USA: AIAA, 2009.

[11] STONEKING E T. Implementation of Kane′s method for a spacecraft composed of multiple rigid bodies: AIAA-2013-4649[R]. USA: AIAA, 2013.

Mr. **Yang Chaoxing** is a Ph. D. candidate in College of Automation Engineering, Nanjing University of Aeronautics and Astronautics (NUAA). His research focuses on dynamic modeling of complex system, aerial refueling system, flight control system.

Dr. **Yang Yu** is a senior engineer. He is working in Shanghai Institute of Spaceflight Control Technology. His research focuses on dynamic modeling of complex system, flight mechanics, space craft control.

Prof. **Lu Yuping** is working in College of Aeronautics, Nanjing University of Aeronautics and Astronautics (NUAA). His research focuses on dynamic modeling of complex system, flight mechanics, morphing aircraft control, hypersonic aircraft control.

(Executive Editor: Xu Chengting)